

A Transformer Less Grid-Connected Hybrid System Based on the Coupled Inductor Multilevel Inverter

**Arshiya Naaz**

M.Tech,

Dept of PID,

AI-Habeeb College of Engineering & Technology,
Chevalla RR District.**Prof. Kareemulla**

Professor,

Dept of PID,

AI-Habeeb College of Engineering & Technology,
Chevalla RR District.

Abstract:

The Photovoltaic (PV), Wind based power generation systems are popular nowadays. In this Renewable energy based systems the voltage stress across the power devices and leakage current are the major issues in transformer-less grid connected system. To overcome the above drawbacks a hybrid system based on the coupled inductor multilevel inverter based single stage transformer less grid connected system is presented in this paper. To maintain the advantages of the impedance network, only a diode is added in the front of the original topology, to block the leakage current loop during the active vectors and open-zero vectors. On the other hand, the near-state pulse width modulation (NSPWM) technique is applied with one-leg shoot-through zero vectors in order to reduce the leakage current through the conduction path in the duration of changing from and to open-zero vectors. Simultaneously, the leakage current caused by other transitions can also be reduced due to the fact that the magnitude of common-mode voltages is reduced. Simulation results of the transformer less hybrid system are presented.

Index Terms:

Leakage current, photovoltaic (PV) and Wind power system, shoot-through zero vector, single-stage boost inverter, width modulation.

I.INTRODUCTION:

The usage of distributed generation renewable sources such as solar energy, wind energy and fuel energy become more popular because of environment friendly and increasing demand of electric energy, which had been described in [1]. Power electronics converter and inverter (power conditioning unit) plays an important role in connecting distributed generation to the grid supply.

High-performance Multilevel inverter[1] are widely used in various applications such as uninterruptible power supplies, distributed power systems, ac motor drives, and hybrid electric vehicles. However, the traditional voltage-source inverter has major problems: 1) it cannot have an ac output voltage higher than the dc source voltage and can only provide buck dc -ac power conversion; 2) shoot through, generated leg, is forbidden. For applications where a low input by both power switches in a voltage is inverted to a high ac output voltage, an additional dc-dc boost converter is needed to obtain a desired ac output. The additional power converter performs two-stage power conversion with high cost and low efficiency. Unlike traditional voltage source inverters [1], Z-source inverters were proposed in [2] in order to accomplish single-stage power conversion with buck boost abilities. In the Z-source inverter, both of the power switches in a leg can be turned on at the same time and thereby eliminate the dead time. This significantly improves the reliability and reduces the output waveform distortion. Various Zsource inverter topologies have been reported in many different studies. Work on Z-source inverters has focused on pulse-width modulation (PWM) strategies [3], [4], applications [5], [6], modeling and control [7], [8], direct ac-ac converters [9], [10], and other Z-network topologies [11]-[13]. A class of quasi-Z source inverters was proposed in [11], [12] that were designed to overcome the shortcomings of the classic Z-source inverter. Quasi-Z-source inverters have advantages, such as a reduction in the passive component ratings and an improvement in the input profiles. Some papers have recently focused on improving the boost factor of the Z-source inverter by using a very high modulation index in order to achieve an improvement in the output waveform. For instance, studies add inductors, capacitors, and diodes to the Z-impedance network in order to produce a high dc link voltage for the main power circuit from a very low input dc voltage.

In two inductors in the impedance Z-network are replaced by a transformer with a turn ratio of 2:1 in order to obtain a high voltage gain. These topologies suit solar cell and fuel cell applications, since they require a high voltage gain in order to match the source voltage to the line voltage. Applying coupled inductor structures to the dc-dc conversion process provides a high boost in cascade and transformer less structures with a high efficiency and high power density. The coupled inductor provides a strong step-up inversion that overcomes the boost limitations of the Z-source inverter (ZSI) [2]. The embedded Z-source inverter developed in is built by inserting dc sources into the X-shaped impedance network. Because the dc sources connect directly to the impedance network inductors, the dc input current in the embedded Z-source inverter flows smoothly, compared to that found in a traditional Z-source inverter [2].

The embedded Z-source inverter assumes the two sources can produce the same voltage gain as found in a traditional Z -source inverter. The embedded Z -source inverter provides a continuous input current without adding an input passive filter and also a lower voltage on the capacitors. But leakage current will be present when photovoltaic is connected to grid through embedded Z- source inverter. The proposed paper can reduce the system leakage current in a great deal and can meet the VDE0126-1-1 standard. To maintain the advantages of the impedance network, only a diode is added in the front of the original topology, to block the leakage current loop during the active vectors and open-zero vectors. On the other hand, the near state pulse width modulation (NSPWM) technique is applied with one-leg shoot-through zero vectors in order to reduce the leakage current through the conduction path in the duration of changing from and to open-zero vectors. Simultaneously, the leakage current caused by other transitions can also be reduced due to the fact that the magnitude of common-mode voltages is reduced.

II. HYBRID SYSTEM Photovoltaic Module:

The Photovoltaic Module The operation and the performance of PV generator depends to its maximum power, the models describing the PV module’s maximum power output behaviors are more practical for PV system assessment. The following section describes the mathematical model for estimating the power output of PV. The equivalent circuit of a PV cell is shown in Fig 2. It includes a current source, a diode, a series resistance and a shunt resistance [2], [4].

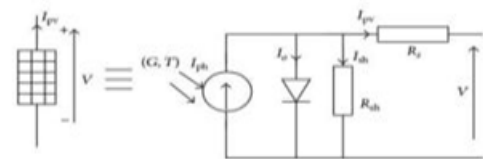


Fig. 2 The equivalent circuit of a PV cell

The current source I_{ph} represents the cell photocurrent. R_{sh} and R_s are the intrinsic shunt and series resistances of the cell, respectively. Usually the value of R_{sh} is very large and that of R_s is very small, hence they may be neglected to simplify the analysis. PV cells are grouped in larger units called PV modules which are further interconnected in a parallelseries configuration to form PV arrays. The photovoltaic panel can be modeled mathematically as given in equations below: Module photo-current:

$$I_{ph} = [ISCr + K_i (T - 298)] * G / 1000 \quad (1)$$

Where I_{ph} is the light generated current in a PV module (A), $ISCr$ is the PV module short-circuit current at 25oC and 1000W/m², K_i is the short-circuit current temperature co-efficient at $ISCr = 0.0017A/oC$, T is the module operating temperature in Kelvin, G is the PV module illumination (W/m²) = 1000W/m².

Module reverses saturation current - I_{rs} :

$$I_{rs} = IScr [exp (VoC NskAT) - 1]$$

Where q is Electron charge = 1.610-19C, V_{oc} is the open circuit voltage, N_s is the number of cells connected in series, k is Boltzman constant = 1.3805*10⁻²³J/K, $A = B$ is an ideality factor = 1.6, The module saturation current I_0 varies with the cell temperature, which is given by

$$I_0 = I_{rs} [T Tr] 3 exp [* Ego Bk [1 Tr - 1 T]]$$

Where T_r is the reference temperature = 298 K, I_0 is the PV module saturation current (A), E_{go} is the band gap for silicon = 1.1 eV. The current output of PV module is Where N_p is the number of cells connected in parallel, V_{pv} is output voltage of a PV module (V), I_{pv} is output current of a PV module (A), R_s is the series resistance of a PV module. Equations (1) - (4) are used to develop the PV model.

The Wind Turbine:

Currently two types of configuration for wind turbine exist, which is the vertical-axis wind turbine (VAWT) configuration and the widely used horizontal axis wind turbine (HAWT) configuration. HAWT have the ability to collect maximum amount of wind energy for time of day and season and their blades can be adjusted to avoid high wind storm. Wind turbines operate in two modes namely constant or variable speed. For a constant speed turbine, the rotor turns at constant angular speed regardless of wind variations. One advantage of this mode is that it eliminates expensive power electronics such as inverters and converters. Its disadvantage however, is that it constrains rotor speed so that the turbine cannot operate at its peak efficiency in all wind speeds. For this reason a constant wind speed turbine produces less energy at low wind speeds than does a variable wind speed turbine which is designed to operate at a rotor speed proportional to the wind speed below its rated wind speed [3]. The output power or torque of a wind turbine is determined by several factors. Among them are (i) turbine speed, (ii) rotor blade tilt, (iii) rotor blade pitch angle (iv) size and shape of turbine, (v) area of turbine, (vi) rotor geometry whether it is a HAWT or a VAWT, (vii) and wind speed. A relationship between the output power and the various variables constitute the mathematical model of the wind turbine. In this paper a model describing HAWT is proposed.

For an object having mass m and velocity V under a constant acceleration, the kinetic energy W_w is given by

$$W_w = 1/2 mv^2 \quad (5)$$

The power P_w in the wind is given by the rate of change of kinetic energy, i.e

$$P_w = dW_w / dt = 1/2 dm / dt V_w^2 \quad (6)$$

But the mass flow rate is given by

$$dm / dt = \rho AV_w \quad (7)$$

Where A is the swept area of the turbine, ρ is the density of air. With this expression equation (7) becomes

$$P_w = 1/2 \rho AV_w^3 \quad (8)$$

The actual mechanical power P_w extracted by the rotor blades in watts is the difference between the upstream and the downstream wind powers [3], i.e.

$$P_w = 1/2 \rho AV_w(V_u^2 - V_d^2) \quad (9)$$

Where V_u is the upstream wind velocity at the entrance of the rotor blades in m/s and V_d is the downstream wind velocity at the exit of the rotor blades in m/s. From the mass flow rate, the equation can be written as

$$\rho AV_w = \rho A(V_u + V_d)^2 \quad (10)$$

V_w being the average of the velocities at the entry and exit of rotor blades of turbine. With this expression, equation (10) can be simplified and becomes

$$P_w = 1/2 \rho AV_w^3 \quad (11)$$

Where C_p is a fraction called the power coefficient. The power coefficient represents a fraction of the power in the wind captured by the turbine and has a theoretical maximum of 0.593. C_p is often called the Betz limit after the Germany physicist Albert Betz who worked it out in 1919. The power coefficient can be expressed by a typical empirical formula

$$C_p = 1/2 (\lambda\lambda - 0.022\beta^2 - 5.6)e^{-0.17} \quad (12)$$

Where β is the pitch angle of the blade in degrees and λ is the tip speed ratio of the turbine, defined as

$$\lambda = V_w \text{ (mph)} / w_b \text{ (rads}^{-1}\text{)} \quad (13)$$

Where w_b is the turbine angular speed. Equations (5) - (13) describe the power captured by the turbine and constitute the turbine model.

III. COUPLED INDUCTOR BASED SINGLE-STAGE BOOST THREE-PHASE MULTI LEVEL INVERTER

The CL-SSBI is shown in Fig. 2. A diode is added in the front of the topology, to block the leakage current loop during the active vectors and open-zero vectors, of which the CMV v_{CM} is defined as

$$v_{CM} = \frac{v_{aN} + v_{bN} + v_{cN}}{3} \quad (1)$$

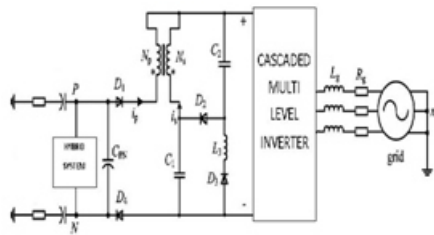


Fig. 1. Transformer less grid-connected Hybrid system based on CL-SSBI with an additional diode

The voltage between positive P or negative N solar panel and grounded neutral n can be expressed as

$$v_{Nn} = -\frac{v_{aN} + v_{bN} + v_{cN}}{3} = -v_{CM} \quad (2)$$

$$v_{Pn} = v_{PN} + v_{Nn} = v_{PN} - v_{CM} \quad (3)$$

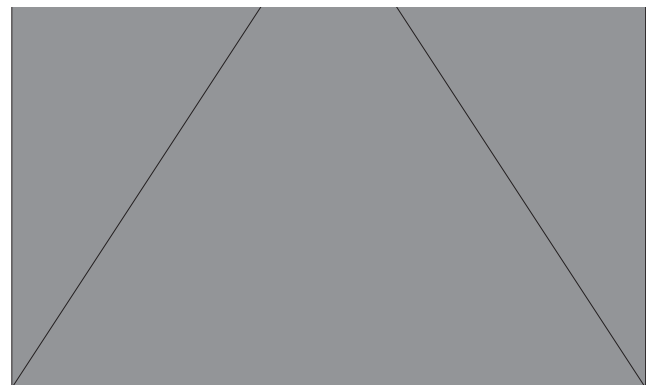
Because shoot-through of the inverter bridge becomes a normal operation state, the possible switching states include six active vectors ($V_1 - V_6$), two open-zero vectors (V_0, V_7), and seven shoot-through zero vectors including one leg shoot through ($V_{a\text{ shoot}}, V_{b\text{ shoot}}, V_{c\text{ shoot}}$), two-legs shoot through ($V_{ab\text{ shoot}}, V_{bc\text{ shoot}}, V_{ca\text{ shoot}}$) and three-legs shoot through ($V_{abc\text{ shoot}}$). For all the odd active vectors (V_1, V_3, V_5), all the even active vectors (V_2, V_4, V_6), all the open-zero vectors (V_0, V_7), and all the shoot-through zero vectors, the common mode voltages (v_{CM}) and voltages (v_{Pn}, v_{Nn}) of CL-SSBI and CL-SSBI with an additional diode (CL-SSBI-D) can be derived from (2) and (3), as shown in Table I. For convenience, supposing the turns ratio N of the coupled inductor is 2.5, shoot-through zero duty cycle D_0 is 0.17, and then boost factor B is 3, according to the bus voltage expression of $V_b = Bv_{PN}$ [16], and using the maximum constant boost (MCB) control method realized by space vector -based PWM control [18], the switching pattern and CMV of CL-SSBI and CL-SSBI-D in section A1 [see Fig. 2(a)] can be obtained, as shown in Fig. 2(b) and (c), in which T_s is defined as a switching period.

Table I Common-Mode Voltages v_{CM} , voltages v_{Nn} and v_{Pn} in different space vectors (a) for CL-SSBI-D (b) for CL-SSBI

space vector	v_{CM}	v_{Nn}	v_{Pn}
V_{odd}	$Bv_{PN}/3$	$-Bv_{PN}/3$	$(1-B/3)v_{PN}$
V_{even}	$\frac{5-N}{6N}Bv_{PN}$	$-\frac{5-N}{6N}Bv_{PN}$	$\frac{6N-(5-N)B}{6N}v_{PN}$
V_0	0	0	v_{PN}
V_7	$\frac{3-N}{2N}Bv_{PN}$	$-\frac{3-N}{2N}Bv_{PN}$	$\frac{2N-B(3-N)}{2N}v_{PN}$
V_{shoot}	0	0	v_{PN}

(b)			
space vector	v_{CM}	v_{Nn}	v_{Pn}
V_{odd}	$Bv_{PN}/3$	$-Bv_{PN}/3$	$(1-B/3)v_{PN}$
V_{even}	$2Bv_{PN}/3$	$-2Bv_{PN}/3$	$(1-2B/3)v_{PN}$
V_0	0	0	v_{PN}
V_7	Bv_{PN}	$-Bv_{PN}$	$(1-B)v_{PN}$
V_{shoot}	0	0	v_{PN}

Table II Simulation And Experimental Parameters Of CL-SSBI And CL-SSBI-D Transformer Less Pv System



In section A1, V_1, V_2, V_0 , and V_7 are used to synthesize the output reference voltage and V_{shoot} is inserted in open-zero vectors to realize the boost characteristics. Fig. 2(b) and (c) illustrates that the magnitude of CMV of CL-SSBI-D is lower than that of CL-SSBI, which indicates that the magnitude of the leakage current can be also reduced.

V. MODULATION TECHNIQUE TO REDUCE LEAKAGE CURRENT

The CMV of CL-SSBI-D changes in a maximum step value when the active vectors V_{odd} convert to open-zero vector V_0 , and changes in a relatively high step value when the open-zero vector V_0 convert to shoot-through zero vectors V_{shoot} , as shown in Fig. 2(c), which will induce high spikes in the leakage current due to the parasitic capacitor path.

Therefore, open-zero vectors are the key to be considered to reduce the magnitude of the leakage current. One possible technique is the NSPWM control, which omits the open-zero vectors and employs three adjacent voltage vectors to synthesize the output reference voltage. V_{shoot} can still be inserted to boost the output voltage. The utilized voltage vectors are changed every 60° throughout the space, as shown in Fig. 3(a).

Compared to the MCB control method [see Fig. 2(a)], the sections rotate 30° in clockwise. Moreover, only one-leg shoot-through vectors are used in order to reduce switching events, and are changed every 120° to assure equal current stress of each leg during shoot-through zero vectors, that is Va shoot for 30° to 150°, Vb shoot for 150° to 180° and -180° to -90°, and Vc shoot for -90° to 30°. The voltage utilization level can be indicated by the modulation index m_i ($m_i = V_m / (2V_b / \pi)$), where V_m is the magnitude of the reference voltage vector). Modulation index within the linear area for NSPWM control is $m_i \pi 3 \sqrt{3}, \pi 2 \sqrt{3} = [0.61, 0.907]$. Therefore, m_i stays in the high modulation index section, leading to lower harmonic distortion of the output waveforms than the remote-state PWM (RSPWM) control [19], which include OPWM and EPWM control. Under the same circuit conditions from Section II and by using the NSPWM control, the switching pattern and CMV of CL-SSBI-D in section B1 and B2 can be obtained, as shown in Fig. 3(b) and (c), in which T_{sh} is defined as a shoot-through period. From Fig. 3(b) and (c), changes of CMV should result in eight spikes in the leakage currents per switching cycle, corresponding

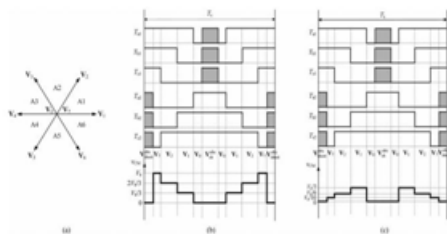


Fig. 2. (a) Voltage space vectors of a three-phase inverter; switching pattern and CMV of (b) CL-SSBI in section A1, and of (c) CL-SSBI-D in section A1.

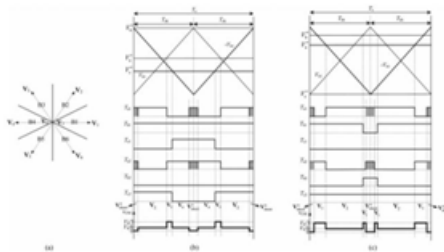


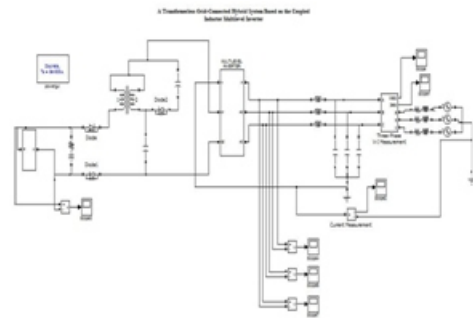
Fig. 3. (a) Voltage space vectors of NSPWM definition; switching pattern and CMV of CL-SSBI-D in (b) section B1 and (c) section B2.

To 1600 spikes in the leakage current per fundamental cycle ($T_s = 100 \mu s$, 50 Hz grid). Nevertheless, the magnitude of the leakage current is lower than that of CL-SSBI with the MCB control method.

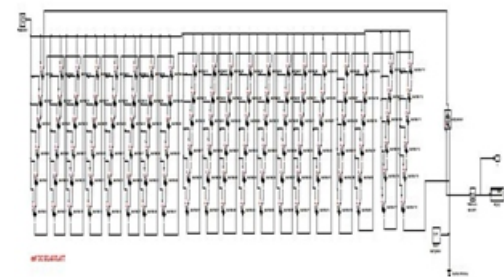
It is important to note that leakage current occurs from CMV only in the duration of transiting from or to shoot-through zero vectors with NSPWM control, when open-zero vectors are omitted. And the magnitude of CMV is also reduced, which leads to lower leakage current.

SIMULATION RESULTS:

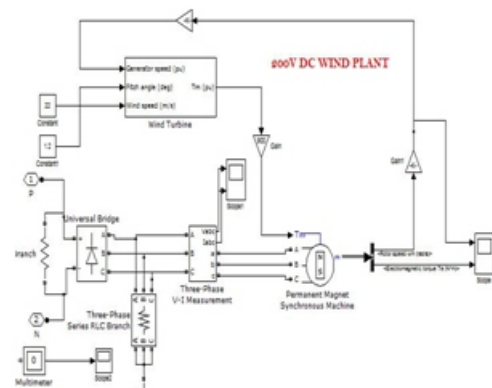
Simulink circuit



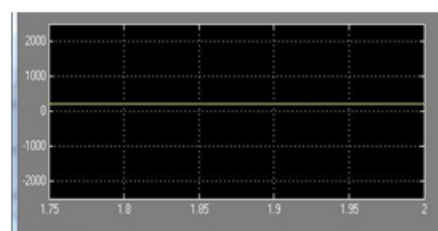
PV System



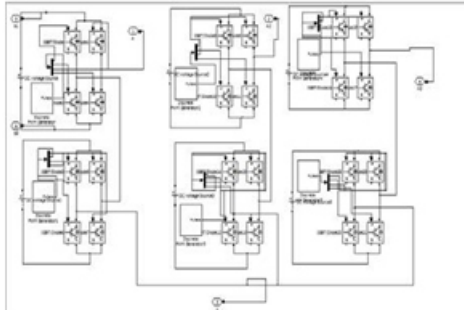
Wind system



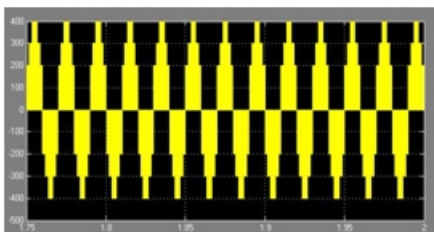
HYBRID SYSTEM OUTPUT



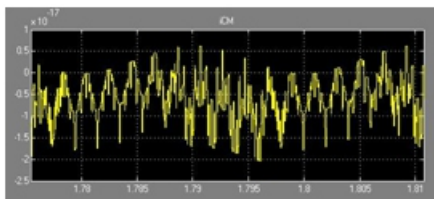
MULTI LEVEL INVERTER



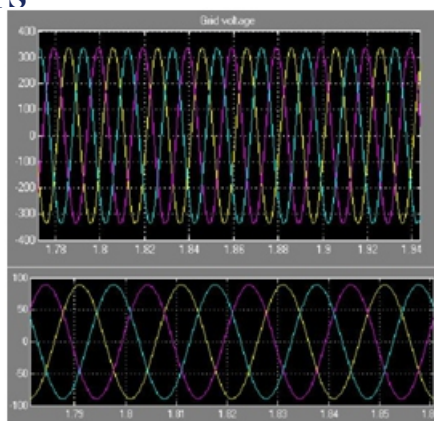
Ph to Ph OUTPUT



Reverse Leakage Currents



GRID CONNECTED VOLTAGE AND CURRENTS



CONCLUSION:

This paper has presented a transformer less grid-connected PV system based on a coupled inductor single-stage boost three phase Multi level inverter. Diode D4 is added in the front of the topology together with D1, to block the leakage current loop during the active vectors and open-zero vectors.

The leakage current caused in the transient states of changing from and to shoot-through zero vectors is also reduced by using the NSPWM technique with one-leg shoot-through zero vectors, when open-zero vectors are omitted. Simultaneously, the leakage current caused by other transitions can be further reduced due to the magnitude reduction of the CMV. The CMVs and the caused leakage currents are compared between CL-SSBI with MCB control and CL-SSBID with NSPWM. According to the simulation and experimental results, the amplitude and RMS value of the leakage current can be well below the threshold level required by the VDE0126-1-1 standards, indicating an effective leakage current reduction.

REFERENCES:

- [1]R. Gonzalez, J. Lopez, P. Sanchis, and L. Marroyo, "Transformer less inverter for single-phase photovoltaic systems," *IEEE Trans. Power Electron.*, vol. 22, no. 2, pp. 693–697, Mar. 2007.
- [2]H. Xiao and S. Xie, "Transformer less split-inductor neutral point clamped three-level PV grid-connected inverter," *IEEE Trans. Power Electron.*, vol. 27, no. 4, pp. 1799–1808, Apr. 2012.
- [3]S. V Araujo, P. Zacharias, and R. Mallwitz, "High efficiency single-phase transformer less inverters for grid-connected photovoltaic systems," *IEEE Trans. Ind. Electron.*, vol. 57, no. 9, pp. 3118–3128, Sep. 2010.
- [4]M. C. Cavalcanti, K. C. de Oliveira, A. M. de Farias, F. A. S. Neves, G. M. S. Azevedo, and F. Camboim, "Modulation techniques to eliminate leakage currents in transformer less three-phase photovoltaic systems," *IEEE Trans. Ind. Electron.*, vol. 57, no. 4, pp. 1360–1368, Apr. 2010.
- [5]J. M. Shen, "Novel transformer less grid-connected power converter with negative grounding for photovoltaic generation system," *IEEE Trans. Power Electron.*, vol. 27, no. 4, pp. 1818– 1829, Apr. 2012.
- [6]O'Lo'pez, F. D. Freijedo, A. G. Yepes, P. Ferna'ndez-Comesan'a, J.Malvar, R. Teodorescu, and J. Doval-Gandoy, "Eliminating ground current in a transformer less photovoltaic application," *IEEE Trans. Energy Convers.*, vol. 25, no. 1, pp. 140–147, Mar. 2010.

[7]F. Bradaschia, M. C. Cavalcanti, P. E. P. Ferraz, F. A. S. Neves, E. C. dos Santos, Jr., and J. H. G. M. da Silva, "Modulation for three-phase transformer less Z-source inverter to reduce leakage currents in photovoltaic systems," *IEEE Trans. Ind. Electron.*, vol. 58, no. 12, pp. 5385–5395, Dec. 2011.

[8]X. Guo, M. C. Cavalcanti, A. M. Farias, and J. M. Guerrero, "Singlecarrier modulation for neutral point-clamped inverters in three-phase transformer less photovoltaic systems," *IEEE Trans. Power Electron.*, vol. 28, no. 6, pp. 2635–2637, Jun. 2013.

[9]I. Patrao, E. Figueres, F. Gonzalez-Espin, and G. Garcia, "Transformer less topologies for grid-connected single-phase photovoltaic inverters," *Renewable Sustainable Energy Rev.*, vol. 15, no. 7, pp. 3423–3431, Sep. 2011.

[10]D. Barater, G. Buticchi, A. S. Crinto, G. Franceschini, and E. Lorenzani, "Unipolar PWM strategy for transformer less PV grid-connected converters," *IEEE Trans. Energy Convers.*, vol. 27, no. 4, pp. 835–843, Dec. 2012.

[11]M. C. Cavalcanti, A. M. Farias, K. C. de Oliveira, F. A. S. Neves, and J. L. Afonso, "Eliminating leakage currents in neutral point clamped inverters for photovoltaic systems," *IEEE Trans. Ind. Electron.*, vol. 59, no. 1, pp. 435–443, Jan. 2012.

[12]T. Salmi, M. Bouzguenda, A. Gastli, and A. Masmoudi, "Transformer less micro inverter for photovoltaic systems," *Int. J. Energy Environ.*, vol. 3, no. 4, pp. 639–650, Jan. 2012.

[13]B. Yang, W. H. Li, Y. J. Gu, W. F. Cui, and X. N. He, "Improved transformer less inverter with common-mode leakage current elimination for a photovoltaic grid-connected power system," *IEEE Trans.* vol. 27, no. 2, pp. 752–762, Feb. 2012.

[14]B. Gu, J. Dominic, J.-S. Lai, C.-L. Chen, T. LaBella, and B. Chen, "High reliability and efficiency single-phase transformer less inverter for grid connected photovoltaic systems," *IEEE Trans. Power Electron.*, vol. 28, no. 5, pp. 2235–2245, May 2013.

[15]E. Koutroulis and F. Blaabjerg, "Design optimization of transformer less grid-connected PV inverters including reliability," *IEEE Trans. Power Electron.*, vol. 28, no. 1, pp. 325–335, Jan. 2013.

[16]Y. Zhou and W. Huang, "Single-stage boost inverter with coupled inductor," *IEEE Trans. Power Electron.*, vol. 27, no. 4, pp. 1885–1893, Apr. 2012.

[17]F. Z. Peng, "Z-source inverter," *IEEE Trans. Ind. Appl.*, vol. 39, no. 2, pp. 504–510, Mar. 2003.

[18]M. Shen, J. Wang, A. Joseph, F. Z. Peng, L. M. Tolbert, and D. J. Adams, "Constant boost control of the Z-source inverter to minimize current ripple and voltage stress," *IEEE Trans. Ind. Appl.*, vol. 42, no. 3, pp. 770–778, 2006.

Author's Details:

Arshiya Naaz received her B.Tech. Degree in Electrical & Electronics Engineering from Jawaharlal Nehru Technological University, Hyderabad, India in 2013. Currently, she is pursuing M.Tech. Degree in power and industrial drives from Al-Habeeb college of Engineering and technology, Hyderabad, India. Chevella, Telangana, India.

Sri.Karimulla Peerla Shaik received his B.Tech. Degree in Electrical & Electronics Engineering from Jawaharlal Nehru Technological University, Hyderabad, India, 2006 & M.Tech. Degree in Electrical & Electronics Engineering from Jawaharlal Nehru Technological University, Hyderabad, India, in 2011. Currently, he is pursuing Ph.D from Jawaharlal Nehru Technological University, Kakinada, India, and working as an Associate Professor in Al-Habeeb College of Engineering and Technology, Chevella, Telangana, India. He has published a number of papers in various national & international journals & conferences. His research areas are power system economics and optimization.